Effects of tumor necrosis factor-α on *follicular dendritic cell secreted protein* (*FDC-SP*) gene transcription in gingival epithelial cells, and localization and expression pattern of FDC-SP in the junctional epithelium of inflamed gingiva

（歯肉上皮細胞における FDC-SP 遺伝子の転写に対する TNF-α の効果と炎症性歯肉の接合上皮における FDC-SP の局在と発現変化）

日本大学大学院松戸歯学研究科歯学専攻

岩井　泰伸

（指導:　小方　賴昌　教授）

Preface

This article is based on a main reference paper, “Tumor necrosis factor-α regulates human follicular dendritic cell secreted protein gene transcription in gingival epithelial cells’’ in the Genes to cells, and a reference paper, “Localization and expression pattern of amelotin, odontogenic ameloblast-associated protein and follicular dendritic cell-secreted protein in the junctional epithelium of inflamed gingiva’’ in the Odontology.

Abstract

Follicular dendritic cell secreted protein (FDC-SP) is a secreted protein expressed in follicular dendritic cells, periodontal ligament and junctional epithelium (JE). To elucidate the transcriptional regulation of the human *FDC-SP* gene by tumor necrosis factor-α (TNF-α), we conducted real-time PCR, Western blotting, transient transfection analyses with chimeric constructs of the *FDC-SP* gene promoter linked to a luciferase (LUC) reporter gene, gel mobility shift and chromatin immunoprecipitation assays using Ca9-22 gingival epithelial cells. TNF-α (10 ng/ml) induced *FDC-SP* mRNA and protein levels at 3 h and reached maximum at 12 h. In transient transfection assays, TNF-α (12 h) increased the LUC activities of constructs between -116*FDCSP* and

-948*FDCSP* including the human *FDC-SP* gene promoter. Transcriptional stimulations by TNF-α were partially inhibited in the -345*FDCSP* constructs that included 3-bp mutations in the *YY1*, *GATA*, *CCAAT-enhancer-binding protein 2* (*C/EBP2*) and *C/EBP3*. Transcriptional activities induced by TNF-α were inhibited by tyrosine kinase, MEK1/2 and phosphoinositide 3-kinase inhibitors. The results of ChIP assays revealed that YY1, GATA and C/EBPβ transcription factors interacted with the *YY1*, *GATA*, *C/EBP2* and *C/EBP3* elements that were increased by TNF-α. These studies demonstrate that TNF-α stimulates human *FDC-SP* gene transcription by targeting *YY1*, *GATA*, *C/EBP2* and *C/EBP3* in the *FDC-SP* gene promoter.

The objective of the second study is to elucidate the localization of amelotin (AMTN), odontogenic ameloblastassociated protein (ODAM) and FDC-SP at the JE in *Porphyromonas gingivalis* and *Aggregatibacter actinomycetemcomitans* infected mice and inflamed and non-inflamed human gingiva. We performed immunostaining to determine the localization and expression pattern of AMTN, ODAM and FDC-SP. AMTN, ODAM and FDC-SP in *A. actinomycetemcomitans* infected mice did not change dramatically compared with non-infected mice. AMTN and FDC-SP expressions were observed stronger in *P. gingivalis* infected mice at early stage. However, at the following stage, the coronal part of the AMTN expression disappeared from the JE, and

FDC-SP expression decreased due to severe inflammation by *P. gingivalis*. ODAM expressed internal and external basal lamina, and the expression increased not only at early stage but also at the following stage in the inflammatory JE induced by *P. gingivalis*. These studies demonstrated that TNF-α stimulates human FDC-SP gene transcription by targeting YY1, GATA, C/EBP2 and C/EBP3 elements in the human FDC-SP gene promoter, and the expression pattern of AMTN, ODAM and FDC-SP at the JE were changed during inflammation process and these three proteins might play an important role in the resistance to inflammation.

Introduction

Chronic periodontitis is an inflammatory disease caused by bacteria, host and environmental factors, and presents symptoms such as swollen and bleeding gum, tooth mobility and alveolar bone resorption which results in tooth loss [1, 2]. It is well known that the removal of periodontal pathogens by plaque control, which is crucial for the maintenance of healthy periodontal tissue, and appropriate immune response to bacterial products, such as lipopolysaccharide (LPS) and proteolytic enzymes, may also be essential to maintain healthy periodontal tissue [3, 4]. In the healthy people, bone is constantly remodeling, which means that osteoclasts-mediated bone resorption is in

balance with osteoblasts-mediated osteogenesis [5]. On the other hand, in periodontitis, the integrated cellular systems are interfered with by many factors including inflammatory cytokines which lead to the dysregulation of remodeling of bone and the consequent loss of periodontium [6, 7].

Follicular dendritic cell secreted protein (FDC-SP) is a small secretory protein expressed by follicular dendritic cells in human tonsils [8, 9]. It has the ability to specifically bind to activated B cells and is implicated as a regulator of B cell responses [8, 10]. FDC-SP is also expressed in the parotid gland, periodontal ligament and junctional epithelium (JE) having similar molecular properties to saliva proteins, statherin and histatin, suggesting it could have an antibacterial activity function [11-13]. Several studies show that overexpression of FDC-SP in periodontal ligament cells could keep fibroblastic character, inhibit osteogenic differentiation and enhance osteoclastogenesis [14-17].

Amelotin (AMTN) is a secreted protein that is expressed by ameloblasts during the maturation stage of enamel formation with very limited sequence similarity to other enamel proteins [18-21]. AMTN expression persists in the JE of gingiva at the erupted molars of mice [18], similar to odontogenic ameloblast-associated protein (ODAM) [20].

JE is the stratified non-keratinizing epithelium that surrounds the tooth like a collar and exists as the base of the gingival sulcus attached to the tooth enamel. Tooth enamel and internal basal lamina of JE are bound to each other by hemidesmosome [22]. It is important for the host defense against periodontopathic bacteria and for periodontal protection [13, 23, 24]. As a complex response to bacterial challenge, JE secretes various cytokines and chemokines and activates the immune defense system. FDC-SP in the JE is temporarily decreased in experimental periodontitis [13, 25]. Therefore, the study of FDC-SP in the JE and periodontal ligament may offer new insights into additional defense mechanisms in the periodontium.

To elucidate the mechanism of transcriptional regulation of human FDC-SP gene by inflammatory cytokine, we investigated the effect of tumor necrosis factor-α (TNF-α) on FDC-SP gene transcription in gingival epithelium cells. In addition, we have analyzed AMTN, ODAM and FDC-SP expressions and localizations in *Porphyromonas gingivalis* and *Aggregatibactor actinomycetemcomitans* induced inflamed gingival tissues from mice periodontitis models and inflamed gingiva from chronic periodontitis patients.

Materials and Methods

Experimental procedures

Cell culture

Human gingival squamous carcinoma epithelial Ca9-22 cells and human parotid gland adenocarcinoma HSY cells or human gingival squamous cell carcinoma-derived Sa3 cells were cultured in alpha-minimum essential medium (α-MEM) or Dulbecco's Modified Eagle Medium (DMEM) containing 10% fetal calf serum (FCS) (Wako, Tokyo Japan) at 37°C in 5% CO_2 and 95% air. The cells were grown to confluence in 60 mm culture dishes in α-MEM including 10% FCS, then cultured for 12 h in α-MEM without FCS, and stimulated with TNF-α (10 ng/ml) (Wako, Tokyo Japan). Total RNA was purified from triplicate cultures at 0, 3, 6, 12 and 24 h following stimulation by TNF-α.

Real-time PCR

Total RNAs were isolated using Isogen II (Wako, Tokyo, Japan) from Ca9-22, Sa3 and HSY cells and used as a template for cDNA synthesis. cDNA was prepared using the PrimeScript RT reagent kit (Takara-Bio, Tokyo Japan). Quantitative real-time PCR was performed using the primer sets,

FDC-SP For; 5'-GCCAGTCACTTGCCATTTCT-3',

FDC-SP Rev; 5’-GGGCAGATTCAGGTATTGGA-3’,

GAPDH For; 5’-GCACCGTCAAGGCTGAGAAC-3’;

GAPDH Rev; 5’-ATGGTGGTGAAGACGCCAGT-3',

using the SYBR Premix Ex Taq II in a TP800 thermal cycler dice real-time system (Takara-Bio, Tokyo, Japan). The amplification reactions were performed in a total volume of 25 μl 2x SYBR Premix Ex Taq II (12.5 μl), 10 μM forward and reverse primers and 50 ng cDNA for *FDC-SP* and 10 ng for *GAPDH*. To reduce variability between replicates, PCR premixes containing all reagents except for cDNA were prepared and aliquoted into 0.2 ml PCR tubes. The conditions for thermal cycling were 10 s at 95°C, 40 cycles of 5 s at 95°C and 30 s at 60°C. Post-PCR melting curves confirmed the specificity of single-target amplification, and the expression of *FDC-SP* relative to *GAPDH* was determined in triplicate.

Western blotting

For the Western blotting analysis, cell lysates of Ca9-22 cells were separated in 12% sodium dodecyl sulfate (SDS)-polyacrylamide gel electrophoresis and transferred to a Hybond 0.2 μm PVDF membrane (GE Healthcare, Pittsburgh, PA, USA). The membrane was then incubated for 3 h with anti-FDC-SP polyclonal antibody

(PAB20711; Abnoba, Taipei City, Taiwan) and anti-α tubulin monoclonal antibody (sc-5286; Santa Cruz Biotechnology, Paso Robles, CA, USA). Anti-rabbit and mouse IgG peroxidase conjugated were used as the secondary antibodies (Sigma-Aldrich, St. Louis, MO, USA). Immunoreactivities were detected using Clarity™ Western ECL Blotting Substrates (Bio-Rad, Hercules, CA, USA).

Luciferase assays

To determine the TNF-α response regions in human *FDC-SP* gene promoter, we prepared chimeric constructs by ligating human *FDC-SP* gene promoters into luciferase reporter plasmid. Various length of human *FDC-SP* gene promoter sequences (-116*FDCSP*; -116~+60, -210*FDCSP*; -210~+60, -345*FDCSP*; -345~+60, -501*FDCSP*; -501~+60, -717*FDCSP*; -717~+60, -948 *FDCSP*; -948~+60) were prepared by PCR amplification. Then, the amplified promoter DNAs were cloned into the Sac I site of the pGL3-basic multi-cloning site. Mutation luciferase constructs, mutation *Ying Yang 1* (*YY1*) (-345*mYY1*; TTgAAgATAgTG), mutation *GATA* (-345*mGATA*; AAAcGcTTcTG), mutation CCAAT enhancer binding protein 2 *(C/EBP)2* (-345*mC/EBP2*; CAATGtAtCAgCAA), mutation *C/EBP3* (-353*mC/EBP3*; GCTTcGtAATgGGT), double mutation in *C/EBP2* and *C/EBP3* (-353*mC/EBP2+mC/EBP3*) were made using

the Quickchange Site-directed Mutagenesis Kit (Stratagene, La Jolla, CA, USA) within the context of the homologous -345~+60 *FDC-SP* promoter fragments. All constructs were sequenced as described previously to verify the fidelity of the mutagenesis.

Exponentially growing Ca9-22 cells were used for transient transfection assays. Twenty-four hours after plating, cells at 60-70% confluence were transfected using Lipofectamine 2000 (Invitrogen, Carlsbad, CA, USA). The transfection mixture included 1 μg of luciferase (LUC) plasmid and 2 μg of β-galactosidase (β-Gal) plasmid (Promega, Madison, WI, USA) as an internal transfection control. β-Gal activities were determined separately to normalize the LUC activities. Two days after transfection, the cells were cultured in α-MEM without FCS for 12 h, and then stimulated with TNF-α (10 ng/ml) for 12 h prior to harvest. The luciferase activities were measured using a luminescence reader (AcuuFlex Lumi 400; Aloka, Tokyo, Japan). Protein kinase C (PKC) inhibitor H7 (5 μM), protein kinase A (PKA) inhibitor KT5720 (100 nM), tyrosine kinase inhibitor herbimycin A (HA; 1 μM), mitogen-activated protein kinase (MEK1/2) inhibitor U0126 (5 μM), and phosphoinositide 3-kinase (PI3K) inhibitor LY249002 (10 μM) were used for protein kinases inhibition.

Gel shift analyses

Confluent Ca9-22 cells were stimulated by TNF-α (10 ng/ml) for 0, 3, 6 and 12 h in α-MEM without FCS, and were subsequently used to prepare the nuclear extracts. Double-stranded oligonucleotides encompassing the 5'-Cy5-labeled *YY1*, *GATA*, *C/EBP2* and *C/EBP3* sequences in the human *FDC-SP* gene promoter were prepared. Nuclear proteins (3 μg) were incubated for 20 min at room temperature with 2 pM Cy5-labeled double-stranded oligonucleotide in buffer containing 50 mM KCl, 0.5 mM EDTA, 10 mM Tris-HCl (pH 7.9), 1 mM dithiothreitol, 0.04% Nonidet P-40, 5% glycerol and 1 μg of poly(dIdC). After incubation, the DNA-protein complexes were separated by electrophoresis in 5% non-denaturing acrylamide gels run at 200 V at room temperature. After electrophoresis, the gels were scanned using a Typhoon TRIO+ Variable Mode Imager (GE Healthcare). For competition experiments, 40-fold molar unlabeled oligonucleotides of *YY1*, *GATA*, *C/EBP2* and *C/EBP3* were used. The double-stranded oligonucleotide sequences were:

YY1 For; 5'-CCAATTTCAACATATTGAGATAGTTGA-3',

YY1 Rev; 5'-GATCTCAACTATCTCAATATGTTGAAATTG-3',

GATA For; 5'-CCACAAAAGATTTTGGTATTTA-3',

GATA Rev; 5'-GATCTAAATACCAAAATCTTTTGTG-3',

C/EBP2 For; 5'-CGTAGACCAATGGAGCAACAACATGTA-3',

C/EBP2 Rev; 5'-GATCTACATGTTGTTGCTCCATTGTCTACG-3',

C/EBP3 For; 5'-CAATATGCTTTGCAATAGGTTATAAT-3',

C/EBP3 Rev; 5'-GATTATAACCTATTGCAAAGCATATT-3'.

Chromatin immunoprecipitation (ChIP) assays

To identify interaction between specific transcription factors and DNA *in vivo* in the human *FDC-SP* gene promoter, ChIP assays were carried out using Ca9-22 cells. Confluent Ca9-22 cells in 100 mm culture dishes were stimulated by TNF-α (10 ng/ml) for 0, 3, 6, 12 and 24 h, and then the cells were fixed with 100 μl formaldehyde for 10 min to crosslink the protein-DNA complexes. The fixed cells were rinsed twice by a wash buffer (1 mM phenylmethylsulfonyl fluoride (PMSF) and complete protease inhibitor cocktail (Sigma-Aldrich) in the PBS (-)) on ice, collected by scrape and centrifuged for 5 min at 4 °C. After the cells were resuspended by SDS buffer (1% SDS, 0.01 M EDTA, 0.05 M Tris-HCl, pH 8.1), lysate was sonicated to shear the protein-fragmentary DNA complexes. Sonicated cell supernatants were diluted in a 10-fold ChIP buffer (0.01% SDS, 1. % Triton X-100, 1.2 l M EDTA, 16.7 mM Tris-HCl, pH 8.9, 16.7 mM NaCl, 1 mM PMSF and complete protease inhibitor cocktail in ddH_2O). The diluted supernatants were assigned Input as a control which included

non-specific protein-DNA complexes, and pre-cleared with 80 µl salmon sperm DNA/Protein A-Agarose (50 % Slurry) for 30 min at 4 °C with gentle agitation. For the immunoprecipitation of protein-DNA complexes, 2 µg of rabbit polyclonal anti-YY1 antibody (ab38422, Abcam), GATA-6 (D61E4) XP®Rabbit mAb (#5851, Cell Signaling, Danvers, MA, USA), C/EBPβ (⊿198) (sc-746, Santa Cruz Biotechnology) and the appropriate normal rabbit IgG (sc-2027, Santa Cruz Biotechnology) were used for 300 µl of precleared supernatant, incubated overnight at 4 °C with constant rotation. Sixty µl of salmon sperm DNA/Protein A-Agarose (50 % Slurry) was added for 1 h at 4 °C with rotation to collect the antibody/histone complexes and pellet agarose by gentle centrifugation (1,000 rpm for 1 min). After removing the supernatant that contained unbound chromatin, the pellet was washed with 1 ml each of Low Salt buffer (0.1 % SDS, 1% Triton-X, 2 mM EDTA, 20 mM Tris-HCl, pH 8.1, 150 mM NaCl in ddH2O), High Salt buffer (0.1% SDS, 1% Triton-X-100, 2 mM EDTA, 20 mM Tris-HCl, pH 8.1, 500 mM NaCl in ddH_2O), LiCl buffer (0.25 M LiCl, 0.1% NP-40, 1% deoxycholate, 0.5 mM EDTA, 0.01 M Tris-HCl, pH 8.1 in ddH_2O), and 1 ml of TE buffer (10 mM Tris–HCl, pH 8.1, 1 mM EDTA in ddH_2O) twice. After the TE buffer was removed, Protein A-Agarose/antibody/chromatin complexes were resuspended in a 250 µl elution buffer (1% SDS and 0.1 M $NaHCO_3$ in ddH_2O) and incubated at RT for 15 min with gentle

rotation. After the spin down of the agarose beads, 20 µl 5 M NaCl was added to the supernatant for reverse cross-links, and 10 µl 0.5 M EDTA, 20 µl 1 M Tris-HCl, pH 6.5, and 1 µl 10 mg/ml proteinase K were added to the degradation of the antibodies and proteins. DNA was recovered by phenol/chloroform/isoamylalcohol extraction and ethanol precipitation. The purified DNA was subjected to PCR amplification (1 cycle, 95 °C for 3 min; amplification was performed for 35 cycles, denature at 95 °C for 15 s, anneal at 59 or 60 °C for 15 s, and extend at 72 °C for 1 min; final extension was at 72 °C for 1 min) mainly for the *YY1*, *GATA,C/EBP2* and *C/EBP3* sites within the human *FDC-SP* promoter using *YY1* ChIP For; 5'-GTATTTGGTAGTTTCTAGGA-3',

YY1 ChIP Rev; 5'-GGCTTAAAGGCCTCTCCCCT-3',

GATA ChIP For; 5'-CATGTAAAGTGATAAACTTC-3',

GATA ChIP Rev; 5'-GGGGAATAACCAATGTTTAG-3',

C/EBP2 ChIP For; 5'-CCAGTAAAATGCTTAGAGGT-3',

C/EBP2 ChIP Rev; 5'-CTCCAAATTTTGTGTCTTGT-3',

C/EBP3 ChIP For; 5'-CTTAAGATTCCAGCACTATC-3',

C/EBP3 ChIP Rev; 5'-CTCACAATTTTTTCCTTTAC-3' primers.

KAPA Taq^{TM} Extra HotStart was utilized for the PCR procedure and the PCR products were separated on 2% agarose gels and visualized with ultraviolet light.

Preparation of *P. gingivalis* and *A. actinomycetemcomitans* infected mice for histological analysis

Hemimandibulars with gingival tissues from *P. gingivalis* or *A. actinomycetemcomitans* infected mice were used as periodontitis models. Periodontitis model mice were daily administered 10^9 CFU of *P. gingivalis* (W381) or *A. actinomycetemcomitans* (ATCC700685) suspended in 100 μl of phosphate buffered saline with 2% carboxymethylcellulose via oral topical application for a total of 15 inoculations [26]. Then, they were sacrificed 1 day (early stage) or 30 days (following stage) after the end of infection by *P. gingivalis* as well as 30 days after the end of infection by *A. actinomycetemcomitans*. To investigate the effects of short time inoculations of *P. gingivalis* on the localization of JE related genes, we created periodontitis mice which were infected by *P. gingivalis* for 8 days, they were then sacrificed 1 day after the end of inoculation. Hemimandibulars of the mice were fixed in a 4% paraformaldehyde phosphate buffer solution (Nacalai, Tesque, Inc. Kyoto, Japan) at 4 ºC for 12 h, rinsed with PBS for 24 h at 4 ºC, demineralized with 12.5% EDTA (pH 7.2) for 10 days with daily solution changes, dehydrated through graded ethanol series and embedded in paraffin. We performed sectioning by a thickness of 4 μm from the apical part to the tip

of the incisor, and used the frontal sections of second molars, which had ameloblast layers adjacent to the enamel space at the maturation stage of the incisor, for Hematoxylin-Eosin (HE) staining and immunohistochemistry. Experiments were performed more than three times from three mice in each group.

HE stain analysis

HE staining was performed by using gingival tissues from *P. gingivalis* or *A. actinomycetemcomitans* infected mice as periodontitis modes. The sectioned tissues on the slide glass were deparaffinized by immersing them into xylene three times for 3 min each, and then rehydrating them through graded ethanol series and dH_2O. The tissues were stained by hematoxylin for 2 min and eosin for 1 min, and then immersed them into 0.1% acetic acid twice for 10 sec each. Dehydration was completed through graded ethanol series and xylene, then mounted with Permount mounting. Images were captured with an Olympus DP71 digital camera mounted on an Olympus BX51 microscope (Olympus, Tokyo, Japan).

Immunohistochemistry

We used the same mice that were assigned to HE stain analysis in this study for

immunohistochemistry. The properly comparative sections to this experiment were decided based on the results of HE stain analysis. After they were deparaffinized and rehydrated, antigen activation was completed by immersing the tissues into a boiled citrate buffer (10mM citric acid, 0.05% Tween20, pH6.0) for 20 min. The tissues were rinsed by a wash buffer (1xTBS solution), blocked for 5 min, treated with a primary antibody diluted buffer (50 mM Tris-HCl pH7.2, 1% BSA) for 1 h, and followed by incubations with a secondary antibody for 30 min in these immunohistochemical analyses (EnVision + System HRP Labelled Polymer Anti-Rabbit, DAKO or EnVision + System HRP Labelled Polymer Anti-Mouse) for detection. For the mice tissues, we used anti-AMTN rabbit polyclonal (dilution 1:500), anti-ODAM mouse monoclonal (Dr. A. Nanci, Université de Montréal, QC; dilution 1:4000), anti-FDC-SP rabbit polyclonal (Dr. T. Shinomura, dilution 1:1000), anti-cytokeratin 19 (CK19) mouse monoclonal (ab7755, Abcam, dilution 1:200), and anti-cluster of differentiation 68 (CD68) mouse monoclonal [(KP1), ab955, Abcam, dilution 1:400] antibodies. Following color development with diaminobenzidine (DAB), sections were counterstained with methyl green (S1962, DAKO) and mounted. Images were captured similarly to the HE stain experiment.

Statistical analysis

Triplicate samples were analyzed for each experiment, and experiments were replicated to ensure the consistency of the responses to drugs. Significant differences between the control and treatment groups were determined using the one-way ANOVA and Student's t-test.

Results

Effects of TNF-α on FDC-SP mRNA and protein levels in Ca9-22 cells

To investigate the regulation of *FDC-SP* transcription by TNF-α, we performed real-time PCR using total RNA extracted from human gingival epithelial Ca9-22 and Sa3 cells, and human parotid gland adenocarcinoma-derived epithelial-like HSY cells. Firstly, the dose-response effect of TNF-α on the *FDC-SP* mRNA levels were studied by treating the Ca9-22 cells with different concentrations of TNF-α for 12 h. TNF-α increased *FDC-SP* mRNA levels by dose-dependent manner and had a maximal at 10 ng/ml (Fig. 1A). Treatment of Ca9-22 and Sa3 cells with TNF-α (10 ng/ml) up-regulated *FDC-SP* mRNA levels at 3 h, reached maximum at 12 h and then decreased at 24 h (Fig. 1B, C). TNF-α increased AMTN mRNA levels time-dependent manner at 3 h and reached maximum at 12 and 24 h in HSY cells (Fig. 1D). TNF-α (10

ng/ml) induced FDC-SP protein expression at 3 h and reached its maximum at 12 and 24 h in Ca9-22 cells (Fig. 2).

Luciferase analyses of human *FDC-SP* promoter constructs

As the effect of TNF-α likely involved transcription factor interaction in the promoter region of the human *FDC-SP* gene, subsequent studies were performed. Transient transfection of chimeric constructs encompassing different regions of the human *FDC-SP* gene promoter ligated to a luciferase reporter gene (-116*FDCSP*; -116~+60, -210*FDCSP*; -210~+60, -345*FDCSP*; -345~+60, -501*FDCSP*; -501~+60, -717*FDCSP*; -717~+60, -948*FDCSP;* -948~+60) was performed in Ca9-22 cells. The results of the luciferase assays indicated an increase in transcription after 12 h of treatment with TNF-α (10 ng/ml) in -116*FDCSP* to -948*FDCSP* (Fig. 3). Unique sequences within the human *FDC-SP* gene promoter between -356 to -1, are a *Yin Yang 1* (*YY1*; nts -69 to -53), inverted *CCAAT* (nts -92 to -81), *GATA* (nts -122 to -106), *CCAAT*-enhancer-binding protein 1 (*C/EBP1*; nts -143 to -133), *octamer-binding protein 1* (*Oct1*; nts -159 to -146), *C/EBP2* (nts -194 to -181), *cAMP response element* (*CRE*; nts -224 to -213) and *C/EBP3* (nts -282 to -269) elements (Fig. 4). Next, we introduced 3-bp mutations within the -345*FDCSP* constructs in the *YY1*, *GATA*, *C/EBP2*

and *C/EBP3* elements targeted by TNF-α. When we used mutation -345*FDCSP* constructs, luciferase activities induced by TNF-α were partially inhibited in the -345*mYY1*, -345*mGATA*, -345*mC/EBP2*, -345*mC/EBP3* and double mutation in -345*mC/EBP2* and -345*mC/EBP3* (-345*mC/EBP2*+mC*/EBP3*) (Fig. 5). These results suggested that *YY1*, *GATA*, *C/EBP2* and *C/EBP3* act as functional response elements through which TNF-α regulates *FDC-SP* gene transcription. TNF-α induced -345*FDCSP* activities were inhibited by PKA inhibitor KT5720 (100 nM), tyrosine kinase inhibitor HA (1 μM), MEK1/2 inhibitor U0126 (5 μM) and PI3K inhibitor LY249002 (10 μM). On the other hand, PKC inhibitor H7 (5 μM) could not inhibit the TNF-α induced -345*FDCSP* activity (Fig. 6).

Gel mobility shift assays

To identify nuclear proteins that bind to the *YY1*, *GATA*, *C/EBP2* and *C/EBP3* elements and mediate TNF-α effects on transcription, double-stranded oligonucleotides were Cy5-labeled and incubated with equal amounts (3 μg) of nuclear proteins extracted from confluent Ca9-22 cells that were either not treated (Control) or treated with TNF-α (10 ng/ml) for 3, 6, and 12 h. With the nuclear extract from confluent control culture of Ca9-22 cells, shifts of *YY1*-, *GATA*-, *C/EBP2*- and *C/EBP3*-protein complexes were

evident (Fig. 7, lanes 1, 5, 9 and 13). After stimulation by TNF-α (10 ng/ml), *YY1*-, *GATA*-, *C/EBP2*- and *C/EBP3*-protein complexes were increased at 3 h (Fig. 7, lanes 2, 6, 10 and 14), *YY1*-protein complex reached maximum at 6 and 12 h (Fig. 7, lanes 3 and 4). *GATA*- and *C/EBP3*-protein complexes reached maximum at 6 h (Fig. 7, lanes 7 and 15), *C/EBP2*-protein complex did not increase thereafter (Fig. 7, lanes 11 and 12). When we used the inverted *CCAAT*, *C/EBP1*, *Oct1* and *CRE* as probes (Fig. 4), the DNA-protein complexes did not change after stimulation by TNF-α (data not shown). That these DNA-protein complexes represent how specific interactions were confirmed by competition experiments in a 40-fold molar excess of non-labeled *YY1, GATA, C/EBP2* and *C/EBP3* to reduce DNA-protein complex formations (Fig. 8, lanes 3, 7, 11 and 15). Whereas the *GATA* and *C/EBP2* did not compete with *YY1*- and *C/EBP3*-protein complex formations (Fig. 8, lanes 4 and 16), *YY1* and *C/EBP3* compete with the *GATA* and *C/EBP2*-protein complex formations (Fig. 8, lanes 8 and 12).

Chromatin immunoprecipitation (ChIP) assays

We examined whether transcription factors are able to interact directly with the human *FDC-SP* gene promoter and how TNF-α influences the interactions of these transcription factors with *YY1, GATA, C/EBP2* and *C/EBP3*. To clarify this further, we

used ChIP assays to examine the *in vivo* association of the transcription factors with *YY1, GATA, C/EBP2* and *C/EBP3* elements in Ca9-22 cells. YY1, GATA and C/EBPβ interacted with a chromatin fragment containing the *YY1, GATA, C/EBP2* and *C/EBP3* which were increased by TNF-α (10 ng/ml) in a time dependent manner in Ca9-22 cells (Fig. 9). Next we investigated which signaling pathways can regulate YY1, GATA and C/EBPβ bindings to *YY1, GATA, C/EBP2* and *C/EBP3* after stimulation with TNF-α, tyrosine kinase inhibitor HA, MEK1/2 inhibitor U0126 and PI3K inhibitor LY294002 were used with or without TNF-α treatment. When Ca9-22 cells were stimulated with TNF-α for 12h, YY1, GATA and C/EBPβ binding to *YY1*, *GATA*, *C/EBP2* and *C/EBP3* were almost completely inhibited by three kinase inhibitors (Fig. 10).

Localization of AMTN and ODAM at JE of molars and at the ameloblast layer of the incisor in normal mice

In the histological experiments, first of all, we have confirmed that AMTN and ODAM localize at the JE of the erupted molars and the interface of the ameloblast layer of the mandibular incisor in the maturation stage of amelogenesis, using transverse sections of non-infected mice. The results of the immunohitological analysis showed the localization of AMTN and ODAM at the JE, as shown by arrow (Fig. 11c, d). Then in

the ameloblasts, AMTN and ODAM express at the ameloblast layer facing on the enamel space, namely internal basal lamina of ameloblasts, as showed by arrowheads (Fig. 11f, g). In the enlargement panels, AMTN localized at the internal basal lamina of JE; however, ODAM expresses not only internal basal lamina, but also external basal lamina (Fig. 12k, p). Fifty mM Tris-HCl with 1% BSA without primary antibodies was utilized as the control, which resulted in no signal and suggested that the signal of primary antibodies were specific (Fig. 11b, e).

Localization of AMTN, ODAM and FDC-SP in *P. gingivalis* and *A. actinomycetemcomitans* infected mice gingiva

AMTN and FDC-SP localizations were detected at internal basal lamina of JE in the molars of non-infected mice (Fig. 12k, u). The observation of AMTN and FDC-SP in *A. actinomycetemcomitans* infected mice (Fig.12l, v) did not change dramatically compared with non-infected mice, however both signals AMTN and FDC-SP expressed stronger in *P. gingivalis* infected mice for 8 days and 15 days (survived for 1 day; sacrificed 1 day after the end of infection) (Fig. 12m, n, w, x) than non-infected mice (Fig. 12k, u). In mice infected with *P. gingivalis* for 15 days (survived for 30 days), only the coronal part of AMTN protein expression disappeared from the JE, which

coincidentally happened with the destruction of internal basal lamina due to long periods of inflammation (Fig. 12o). The signal of FDC-SP protein in mice infected with *P. gingivalis* for 15 days (survived for 30 days) (Fig. 12y) was weaker than in mice infected with *P. gingivalis* for 8 days and 15 days (survived for 1 day) (Fig. 12w, x). Localizations of ODAM were also detected in the entire JE of molars, and the signal did not change in *A. actinomycetemcomitans* infected mice (Fig. 12q). However, in *P. gingivalis* infected mice (Fig. 12r, s, t), the signals of ODAM were slightly increased compared to non-infected mice. These findings suggest that AMTN and FDC-SP protein levels were upregulated in the early stage of inflammation, induced by *P. gingivalis*, (Fig. 12m, w). In the late stage the localization of AMTN was limited to the root surface facing the cementum or dentin (Fig. 12o). ODAM protein level also increased, not only at early stage, but also at the late stage in the inflammatory JE induced by *P. gingivalis*.

Discussion

TNF-α is a typical inflammatory cytokine in the inflamed tissues and induces insulin resistance [26]. Adipocytes express high levels of TNF-α [27] and TNF-α serum levels are elevated in obese, type 2 diabetes and cancer patients [28-30]. Periodontitis is an inflammatory disease caused by oral bacteria around the gingival sulci, and severe

periodontitis can result in destruction of periodontium, alveolar bone resorption and tooth loss [31]. Antimicrobial periodontal treatment decreased TNF-α serum levels in chronic periodontitis patients [32, 33]. A positive statistical correlation was detected between the TNF-α concentration in the gingival crevicular fluid and the severity of periodontitis [34]. In this study, we show that TNF-α increases human *FDC-SP* gene transcription temporarily after 12 h in human gingival epithelial cells by targeting *YY1, GATA, C/EBP2* and *C/EBP3* elements in the human *FDC-SP* gene promoter. FDC-SP was identified in primary follicular dendritic cells isolated from human tonsils, having structural similarities to a saliva protein statherin. FDC-SP is also expressed in TNF-α activated FDC-like cell lines and LPS activated peripheral blood leukocytes, but not in B cell lines [8, 9]. Statherin inhibits precipitation from supersaturated calcium phosphate solutions and stabilizes supersaturated saliva [35]. FDC-SP expresses in the periodontal ligament and JE, and prevents mineralization of periodontal ligament and adsorbs onto the surface of enamel and cementum adjacent to JE [12]. FDC-SP in the JE was completely lost 3 h following the treatment with *E. coli* LPS in the upper molars of rats, but the immunoreactivity was detected again after 3 days [13]. The expression of FDC-SP was significantly decreased concurrently with the increase of interleukin-17 (IL-17) at 5 and 7 days after the induction of experimental periodontitis, and FDC-SP

levels had returned to normal at 14 and 28 days [25]. Therefore, to elucidate the function of FDC-SP in the inflamed gingiva, we used TNF-α on *FDC-SP* gene transcription in gingival epithelium cells.

From transient transfection analyses, we initially located the TNF-α response region to the proximal promoter (-116 to +60) of the human *FDC-SP* gene (Fig. 3), which encompasses an *YY1* element (Fig. 4). Transcriptional regulation by TNF-α was partially abrogated when 3-bp mutations within the -345*FDCSP* constructs in the *YY1, GATA, C/EBP2* and *C/EBP3* (Fig. 5). The involvement of *YY1, GATA, C/EBP2* and *C/EBP3* elements is further supported by gel shift assays in which nuclear proteins that formed complexes with *YY1, GATA, C/EBP2* and *C/EBP3* were increased by TNF-α in Ca9-22 cells (Fig. 7). Results of competition gel shift assays confirmed *YY1*-, *GATA*-, *C/EBP2*- and *C/EBP3*-protein complex formations were specific. Interestingly, a 40-fold molar excess of *C/EBP3* competes with *C/EBP2*-protein complex formation, whereas *C/EBP2* could not compete with *C/EBP3*-protein complex formation (Fig. 8), suggesting that the constituents of *C/EBP2*- and *C/EBP3*-binding proteins are not same. YY1 is known to have a fundamental role in normal biologic processes such as differentiation, replication, proliferation and embryogenesis [36]. YY1 plays a critical role in promoting IL-6 transcription in rheumatoid arthritis (RA) which contribute to the

inflammation of RA via stimulation of T helper 17 cell differentiation [37]. GATA transcription factors (GATA-1~6) recognize (A/T)GATA(A/G) motif and GATA-4/5/6 are expressed in the cardiovascular system and in endoderm-derived tissues including the liver, lungs, pancreas and gut [38]. Treatment of mice with LPS led to a transient increase of GATA-6 expression in the liver which was positively correlated with the expression of hepcidin which is upregulated following increased systemic iron concentrations as well as during inflammation [39]. C/EBPs are a family of leucine zipper transcription factors involved in the regulation of various aspects of cellular differentiation and function in a variety of tissues [40]. C/EBPβ was originally identified as a mediator of IL-6 signaling, binding to *IL-6* response elements in the promoters of acute phase response genes *TNF*, *IL-8* and *G-CSF*. TNF-α promotes nuclear localization of C/EBPβ and C/EBPδ in response to inflammatory stress [41]. In this study, we demonstrate that these transcription factors play important roles in transcriptional regulation of human *FDC-SP* gene during the inflammation process.

Results of ChIP assays suggest that TNF-α induced human *FDC-SP* transcription through YY1, GATA and C/EBPβ are targeting *YY1, GATA, C/EBP2* and *C/EBP3* in the human *FDC-SP* gene promoter (Fig. 9). The PKA inhibitor KT5720, tyrosine kinase inhibitor HA, MEK1/2 inhibitor U0126 and PI3K inhibitor LY294002 inhibited the

effects of TNF-α on *FDC-SP* transcription (Fig. 6 and 10), suggesting that PKA, tyrosine kinase, MEK1/2 and PI3K signaling pathways are crucial for TNF-α effects on *FDC-SP* transcription.

In the second study, FDC-SP and AMTN expressions were increased in *P. gingivalis* infected mice at early stage, and then decreased at the following stage due to severe inflammation. The discrepancy of FDC-SP expression after induction of periodontitis in mice might be due to the process generating inflammation and the extent of damage of periodontal tissue. Inflammatory condition was more severely induced by *P. gingivalis* infection compared to *A. actinomycetemcomitans* infection (Fig. 12).

In our previous study, AMTN localization was sparsely penetrated into the connective tissue of the granulation tissue which was removed during periodontal surgery [23]. Whereas in this study, we could not find AMTN in the connective tissue (Fig. 12). It has been reported that AMTN and ODAM expressions at JE regenerate after gingivectomy [42] and AMTN and ODAM interact with each other [43]. These findings might support the localizations and expressions of AMTN, ODAM and FDC-SP at JE even in the process of inflammation could be regulated by some factors from periodontal tissues except for epithelium (Fig. 12).

In conclusion, our study has identified *YY1*, *GATA*, *C/EBP2* and *C/EBP3* elements in the human *FDC-SP* gene promoter that mediate *FDC-SP* transcription induced by TNF-α in gingival epithelial cells and has shown that TNF-α increased YY1, GATA and C/EBPβ binding to the *YY1*, *GATA*, *C/EBP2* and *C/EBP3* elements through the PKA, tyrosine kinase, MEK1/2 and PI3K pathways. Moreover, the localization and expression pattern of AMTN, ODAM and FDC-SP were changed markedly during process of periodontal inflammation at JE. Especially at the internal basal lamina, AMTN was slightly spread and accurately limited along to the long sulcular and junctional epithelium due to the apically epithelium growing in the periodontitis. FDC-SP and AMTN might have a more predominant role in the early stage of inflammation compared to ODAM. Further studies are necessary to explore the precise role of FDC-SP in the JE throughout the progression of periodontitis.

Reference

1. Kinane DF, Attstrom R. (2005) Advances in the pathogenesis of periodontitis. Consensus report. *J Clin Periodontol* **32,** 130-131.

2. Kato A, Imai K, Ochiai K, Ogata Y. (2013) Higher Prevalence of Epstein-barr virus DNA in deeper periodontal pockets of chronic periodontitis in Japanese patients. *PLoS One* **8,** e71990.

3. Netea MG, van Deuren M, Kullberg BJ, Cavaillon JM, Van der Meer JW. (2002) Does the shape of lipid A determine the interaction of LPS with Toll-like receptors? *Trends Immunol* **3,** 135-139

4. Li X, Zhou L, Takai H, Sasaki Y, Mezawa M, Li Z, Wang Z, Yang L, Wang S, Matsumura H, Kaneko T, Yoshimura A, Ogata Y. (2012) Aggregatibacter actinomycetemcomitans Lipopolysaccharide regulates bone sialoprotein gene transcription. *J Cell Biochem* 113, 2822-2834.

5. Nair SP, Meghji S, Wilson M, Reddi K, White P, Henderson B. (1996) Bacterially induced bone destruction : mechanisms and misconceptions. *Infect Immun* **64,** 2371-2380.

6. Diomede F, Zingariello M, Cavalcanti MFXB, Merciaro I, Pizzicannella J, De Isla N, Caputi S, Ballerini P, Trubiani O. (2017) MyD88/ERK/NFkB pathways and pro-inflammatory cytokines release in periodontal ligament stem cells stimulated by Porphyromonas gingivalis. *Eur J Histochem* **61,** 2791.

7. Pihlstrom BL, Michalowicz BS, Johnson NW. (2005) Periodontal diseases. *Lancet* **366,** 1809-1820.

8. Marshall AJ, Du Q, Draves KE, Shikishima Y, HayGlass KT, Clark EA. (2002) FDC-SP, a novel secreted protein expressed by follicular dendritic cells. *J Immunol* **169,** 2381-2389.

9. Nakamura S, Terashima T, Yoshida T, Iseki S, Takano Y, Ishikawa I, Shinomura T. (2005) Identification of genes preferentially expressed in periodontal ligament: specific expression of a novel secreted protein, FDC-SP. *Biochem Biophys Res Commun* **338,** 1197-1203.

10. Al-Alwan M, Du Q, Hou S, Nashed B, Fan Y, Yang X, Marshall AJ. (2007) Follicular dendritic cell secreted protein (FDC-SP) regulates germinal center and antibody responses. *J Immunol* **178,** 7859-7867.

11. Dodds MWJ, Johnson DA, Yeh C-K. (2005) Health benefits of saliva: a review. *J Dent* **33,** 223-233.

12. Shinomura T, Nakamura S, Ito K, Shirasawa S, Hook M, Kimura JH. (2008) Adsorption of Follicular Dendritic Cell-secreted Protein (FDC-SP) onto Mineral Deposits Application of a new stable gene expression system. *J Biol Chem* **283,** 33658-33664.

13. Oshiro A, Iseki S, Miyauchi M, Terashima T, Kawaguchi Y, Ikeda Y, Shinomura T. (2012) Lipopolysaccharade induces rapid loss of follicular dendritic cell-secreted protein in the junctional epithelium. *J Periodont Res* **47,** 689-694.

14. Wei N, Yu H, Yang S, Yang X, Yuan Q, Man Y, Gong P. (2011) Effect of FDC-SP on the phenotype expression of cultured periodontal ligament cells. *Arch Med Sci* **7,** 235-241.

15. Xiang L, Ma L, He Y, Wei N, Gong P. (2013) Osteogenic differentiation of human periodontal ligament cells after transfection with recombinant lentviral vector containing follicular dendritic cell secreted protein. *J Periodont Res* **49,** 554-562.

16. Xiang L, Ma L, He Y, Wei N, Gong P. (2014) Transfection with follicular dendritic cell secreted protein to affect phenotype expression of human periodontal ligament cells. *J Cell Biochem* **115,** 940-948.

17. Liu J, Bian H, Ding R, Chi X, Wang Y. (2016) Follicular dendritic cell-secreted protein may enhance osteoclastogenesis in periodontal disease. *Connect Tissue Res* **57,** 38-43.

18. Iwasaki K, Bajenova E, Somogyi-Ganss E, Miller M, Nguyen V, Nourkeyhani H, Gao Y, Wendel M, Ganss B. (2005) Amelotin-a Novel Secreted, Ameloblast-specific Protein. *J Dent Res* **84,** 1127-1132.

19. Moffatt P, Smith CE, St-Arnaud R, Simmons D, Wright JT, Nanci A. (2006) Cloning of rat amelotin and localization of the protein to the basal lamina of maturation stage ameloblasts and junctional epithelium. *Biochem J* **399,** 37-46.

20. Somogyi-Ganss E, Nakayama Y, Iwasaki K, Nakano Y, Stolf D, McKee MD, Ganss B. (2012) Comparative temporospatial expression profiling of murine amelotin protein during amelogenesis. *Cells Tissues Organs* **195,** 535-549.

21. Lacruz RS, Nakayama Y, Holcroft J, Nguyen V, Somogyi-Ganss E, Snead ML, White SN, Paine ML, Ganss B. (2012) Targeted overexpression of amelotin disrupts the microstructure of dental enamel. *PLoS One* **7,** e35200.

22. Hormia M, Owaribe K, Virtanen I. (2001) The dento-epithelial junction:cell adhesion by type I hemidesmosomes in the absence of a true basal lamina. *J Periodontol* **72,** 788-797.

23. Nakayama Y, Takai H, Matsui S, Matsumura H, Zhou L, Kato A, Ganss B, Ogata Y. (2014) Proinflammatory cytokines induce amelotin transcription in human gingival fibroblasts. *J Oral Sci* **56,** 261-268.

24. Nakayama Y, Matsui S, Noda K, Yamazaki M, Iwai Y, Matsumura H, Izawa T, Tanaka E, Ganss B, Ogata Y. (2016) Amelotin gene expression is temporarily being upregulated at the initiation of apoptosis induced by TGFβ1 in mouse gingival

epithelial cells. *Apoptosis* **21,** 1057-1070.

25. Takahashi S, Fukuda M, Mitani A, Fujimura T, Iwamura Y, Sato S, Kubo T, Sugita Y,

    Maeda H, Shinomura T, Noguchi T. (2014) Follicular dendritic cell-secreted protein is decreased in experimental periodontitis concurrently with the increase of interleukin-17 expression and the Rankl/Opg mRNA ratio. *J Periodontal Res* **49,** 390-397.

26. Uysal KT, Wiesbrock SM, Marino MW, Hotamisligil GS. (1997) Protection from obesity-induced insulin resistance in mice lacking TNF-alpha function. *Nature* **389,** 610-614.

27. Hotamisligil GS, Arner P, Caro JF, Atkinson RL, Spiegelman BM. (1995) Increased adipose tissue expression of tumor necrosis factor-alpha in human obesity and insulin resistance. *J Clin Invest* **95,** 2409-2415.

28. Katsuki A, Sumida Y, Murashima S, Murata K, Takarada Y, Ito K, Fujii M, Tsuchihashi K, Goto H, Nakatani K, Yano Y. (1998) Serum levels of tumor necrosis factor-alpha are increased in obese patients with noninsulin-dependent diabetes mellitus. *J Clin Endocrinol Metab* **83,** 859-862.

29. McCall JL, Tuckey JA, Parry BR. (1992) Serum tumour necrosis factor alpha and insulin resistance in gastrointestinal cancer. *Br J Surg* **79,** 1361-1363.

30. Winkler G, Salamon F, Harmos G, Salamon D, Speer G, Szekeres O, Hajós P, Kovács M, Simon K, Cseh K. (1998) Elevated serum tumor necrosis factor-alpha concentrations and bioactivity in Type 2 diabetics and patients with android type obesity. *Diabetes Res Clin Pract* **42,** 169-174.

31. Kato A, Imai K, Ochiai K, Ogata Y. (2015) Prevalence and quantitative analysis of Epstein - Barr virus DNA and *Porphyromonas gingivalis* associated with Japanese chronic periodontitis patients. *Clin Oral Invest* **19,** 1605-1610.

32. Iwamoto Y, Nishimura F, Nakagawa M, Sugimoto H, Shikata K, Makino H, Fukuda T, Tsuji T, Iwamoto M, Murayama Y. (2001) The effect of antimicrobial periodontal treatment on circulating tumor necrosis factor-alphaand glycated hemoglobin level in patients with type 2 diabetes. *J Periodontol* **72,** 774-778.

33. Iwamoto Y, Nishimura F, Soga Y, Takeuchi K, Kurihara M, Takashiba S, Murayama Y. (2003) Antimicrobial periodontal treatment decreases serum C-reactive protein, tumor necrosis factor-alpha, but not adiponectin levels in patients with chronic periodontitis. *J Periodontol* **74,** 1231-1236.

34. Kurtiş B, Tüter G, Serdar M, Akdemir P, Uygur C, Firatli E, Bal B. (2005) Gingival

crevicular fluid levels of monocyte chemoattractant protein-1 and tumor necrosis factor-alpha in patients with chronic and aggressive periodontitis. J Periodontol **76,** 1849-1855.

35. Schlesinger DH, Hay DI. (1977) Complete covalent structure of statherin, a tyrosine-rich acidic peptide which inhibits calcium phosphate precipitation from human parotid saliva. *J Biol Chem* **252,** 1689-1695.
36. Gordon S, Akopyan G, Garban H, Bonavida B. (2006) Transcription factor YY1: structure, function, and therapeutic implications in cancer biology. *Oncogene* **25,** 1125-1142.
37. Lin J, He Y, Chen J, Zeng Z, Yang B, Ou Q (2016) Datasets of YY1 expression in rheumatoid arthritis patients. *Data in Brief* **9,** 1034-1038.
38. Al-azzeh ED, Fegert P, Blin N, Gött P. (2000) Transcription factor GATA-6 activates expression of gastroprotective trefoil genes TFF1 and TFF2. *Biochim Biophys Acta* **1490,** 324-332.
39. Bagu ET, Layoun A, Calvé A, Santos MM. (2013) Friend of GATA and GATA-6 modulate the transcriptional up-regulation of hepcidin in hepatocytes during inflammation. *Biometals* **26,** 1051-1065.
40. Poli V. (1998) The role of C/EBP isoforms in the control of inflammatory and native

immunity functions. *J Biol Chem* **273,** 29279-29282.

41. Lekstrom-Himes J, Xanthopoulos KG. (1998) Biological role of the CCAAT/enhancer-binding protein family of transcription factors. *J Biol Chem* **273,** 28545-28548.

42. Nishio C, Wazen R, Kuroda S, Moffatt P, Nanci A. (2010) Expression pattern of odontogenic ameloblast-associated and amelotin during formation and regeneration of the junctional epithelium. *Eur Cell Mater* **20,** 393-402.

43. Holcroft J, Ganss B. (2011) Identification of amelotin- and ODAM-interacting enamel matrix proteins using the yeast two-hybrid system. *Euro J Oral Sci* **119,** 301-306.

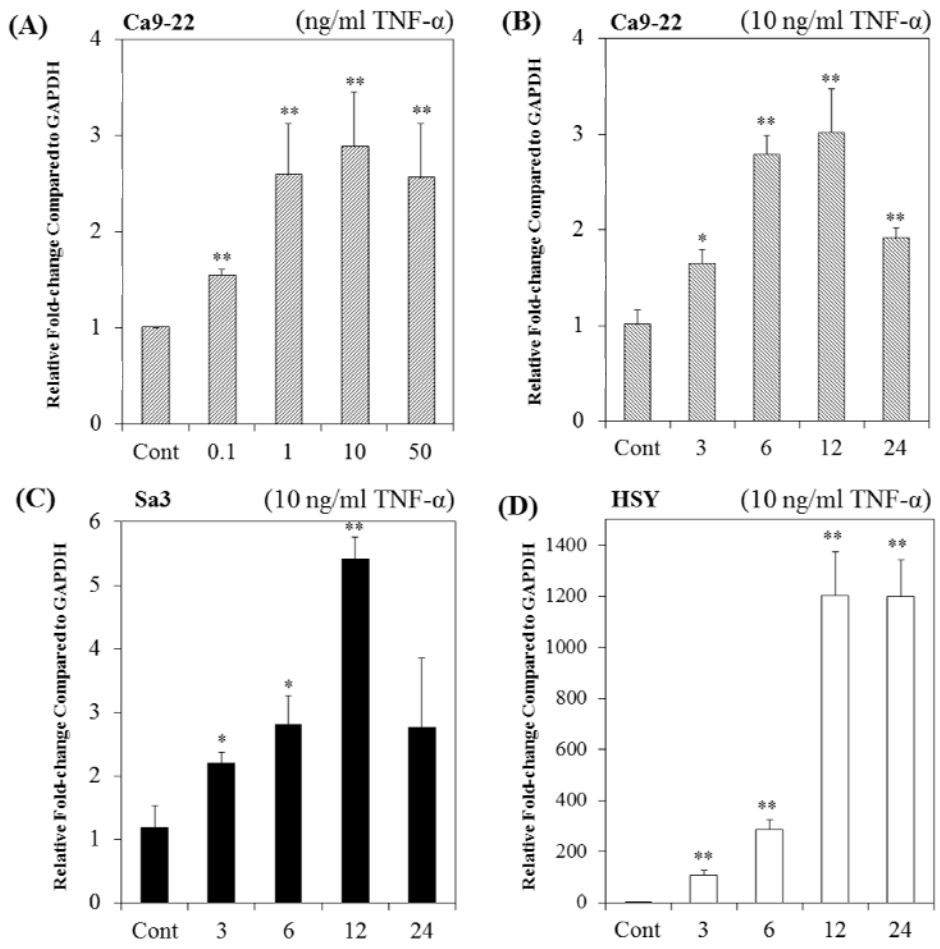

Fig. 1 Effects of TNF-α on *FDC-SP* mRNA levels in Ca9-22, Sa3 and HSY cells. **(A)** Dose-response effects of TNF-α on *FDC-SP* mRNA levels in Ca9-22 cells treated for 12 h. **(B)** Ca9-22 cells were treated with or without TNF-α (10 ng/ml) for 3, 6, 12, and 24 h. **(C)** Sa3 cells were treated with or without TNF-α (10 ng/ml) for 3, 6, 12, and 24 h. **(D)** HSY cells were treated with or without TNF-α (10 ng/ml) for 3, 6, 12, and 24 h. *FDC-SP* and *GAPDH* mRNA levels were measured by real-time PCR. The experiments were performed in triplicate for each data point. Quantitative analyses of the data sets are shown with standard errors. Significantly different from control; *P<0.05 and **P<0.01.

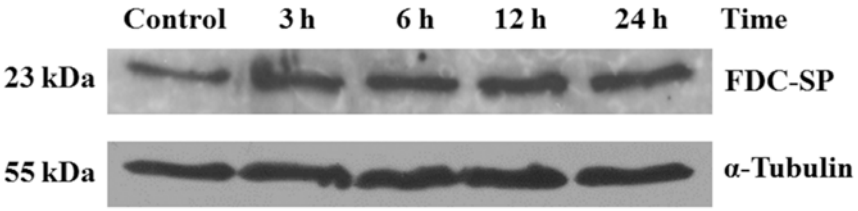

Fig. 2 Effects of TNF-α on FDC-SP protein levels in Ca9-22 cells. FDC-SP protein levels in Ca9-22 cells were analyzed by Western blotting using an anti-FDC-SP, and an anti-α tubulin antibodies.

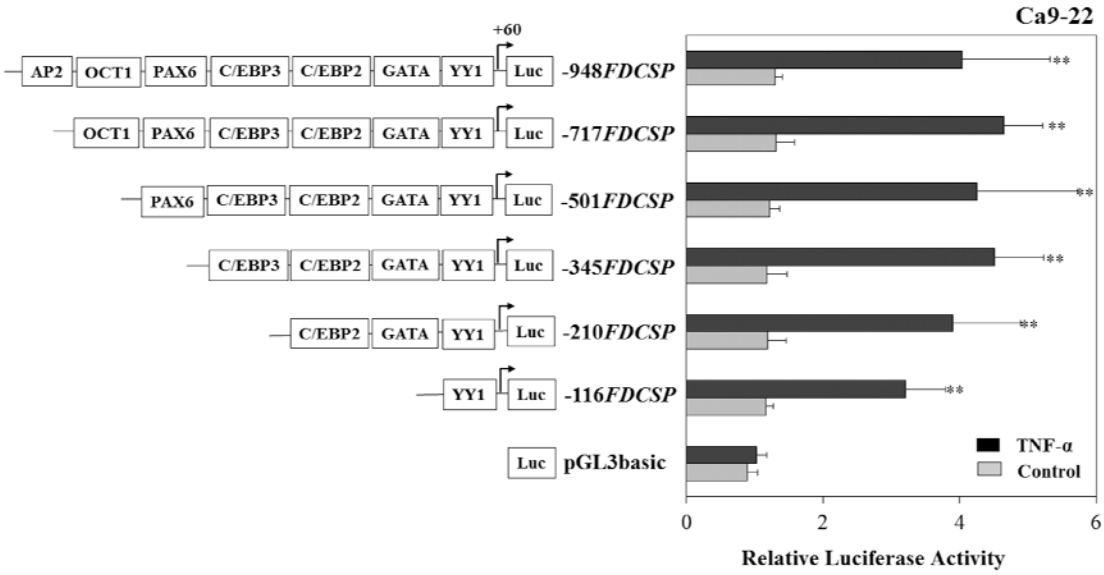

Fig. 3 TNF-α upregulates human *FDC-SP* gene promoter activities. The transcriptional activities of -116*FDCSP* (-116~+60), -210*FDCSP* (-210~+60), -345*FDCSP* (-345~+60), -501*FDCSP* (-501~+60), -717*FDCSP* (-717~+60) and -948*FDCSP* (-948~+60) were increased by TNF-α (10 ng/ml, 12 h) in Ca9-22 cells. Results of transcriptional activities obtained from three separate transfections with constructs, pGL3basic and -116*FDCSP* to -948*FDCSP* were combined and values expressed with standard deviation (SD). **P<0.01

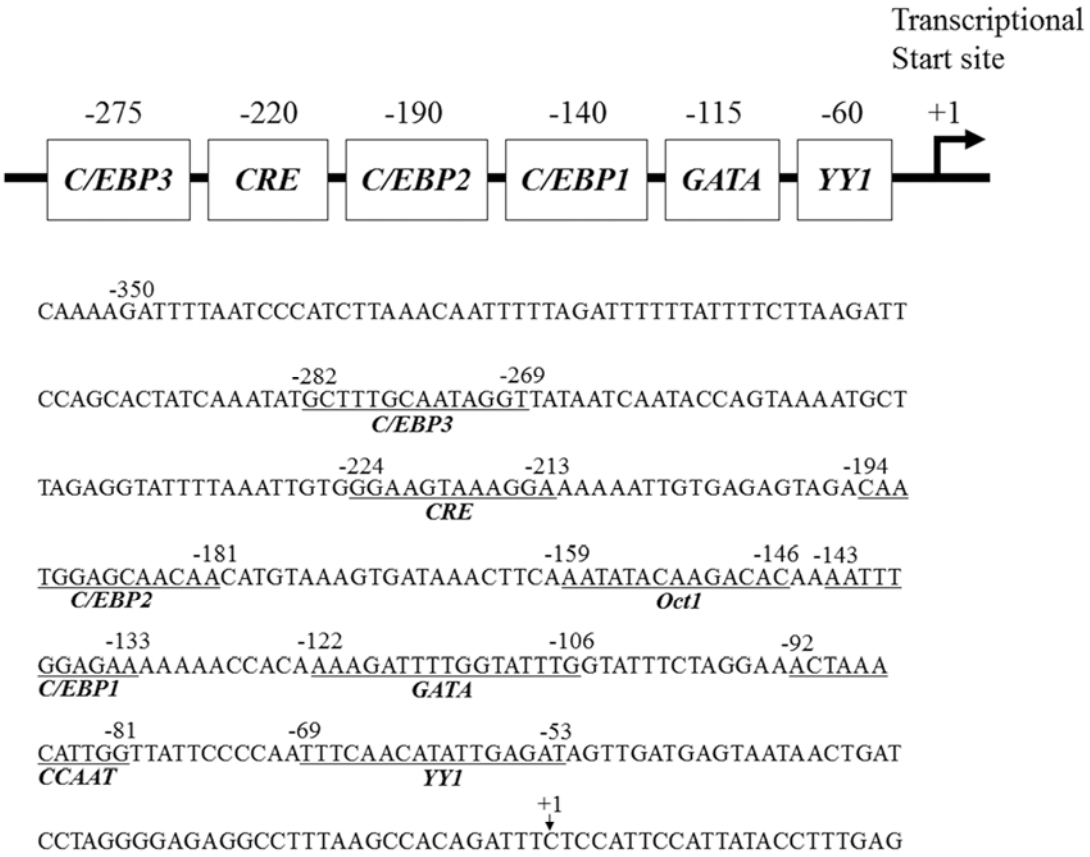

Figure 4 Regulatory elements in the proximal promoter of the human *FDC-SP* gene. **Upper panel:** Positions of the *YY1*, *GATA, C/EBP1*, *C/EBP2, CREB* and *C/EBP3* are shown in the proximal promoter region of the human FDC-SP gene. **Lower panel:** The nucleotide sequence of the human *FDC-SP* gene proximal promoter are shown from -355 to +23. The numbering of nucleotides is relative to the transcription start site (+1).

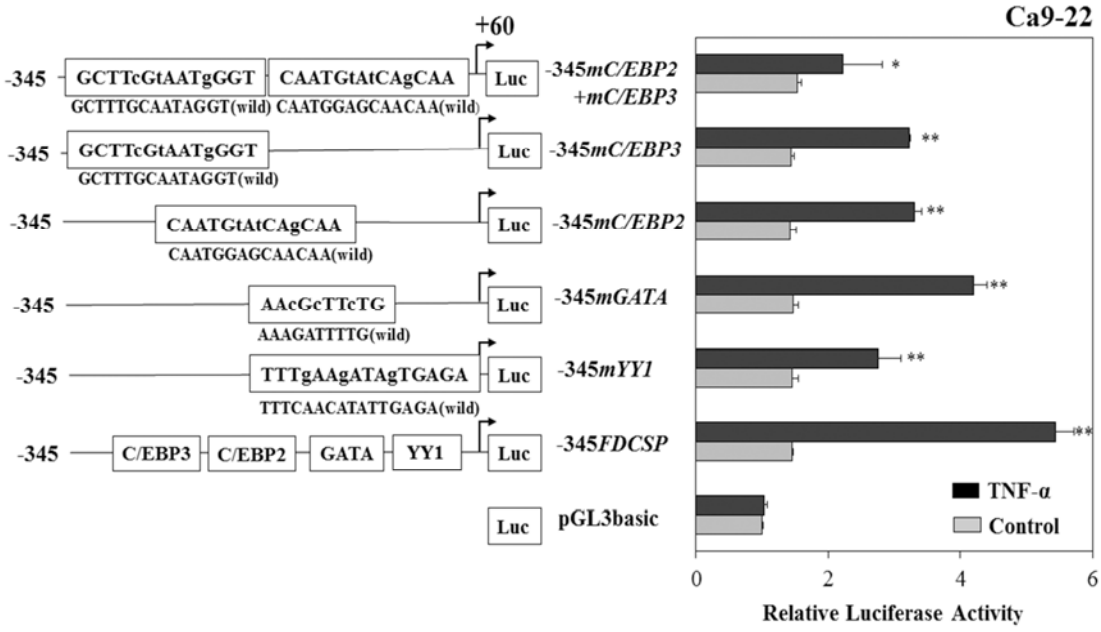

Figure 5 Site-specific mutation analyses of luciferase activities in Ca9-22 cells. After introducing 3-bp mutations, transcriptional induction by TNF-α (10 ng/ml) was partially inhibited in the -345*mYY1*, -345*mGATA*, -345*mC/EBP2*, -345*mC/EBP3* and -345*mC/EBP2+mC/EBP3*. The results of the transcriptional activities obtained from three separate transfections with constructs were combined and the values were expressed with SD. Significantly different from control, *P<0.05 and **P<0.01.

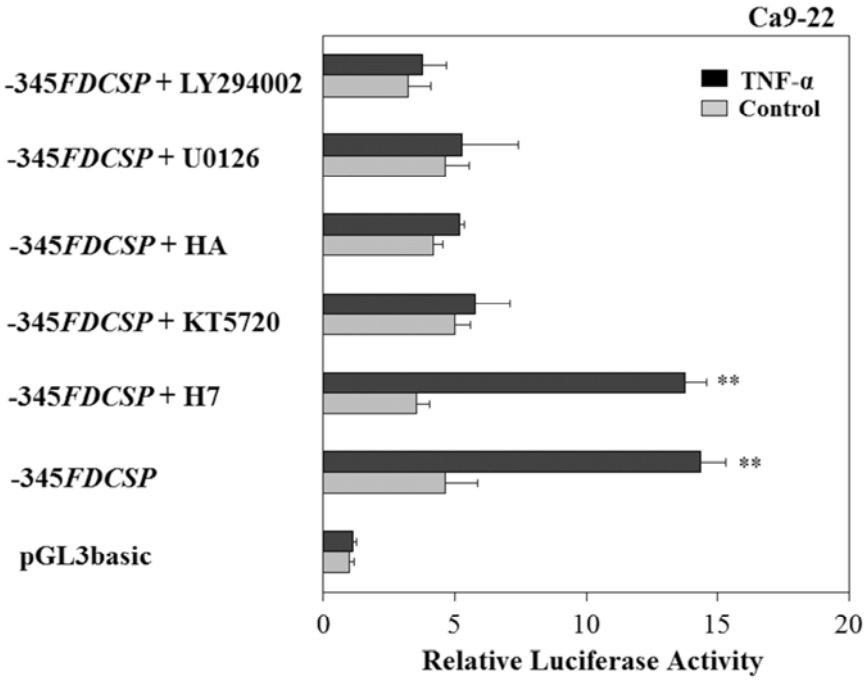

Fig. 6 Effects of kinase inhibitors on transcriptional activation by TNF-α. TNF-α-induced -345*FDCSP* activities were inhibited by KT5720, HA, U0126 and LY294002, and no effect was observed for H7. The results of transcriptional activities obtained from three separate transfections with constructs were combined and values expressed with SD. Significantly different from control, **P<0.01.

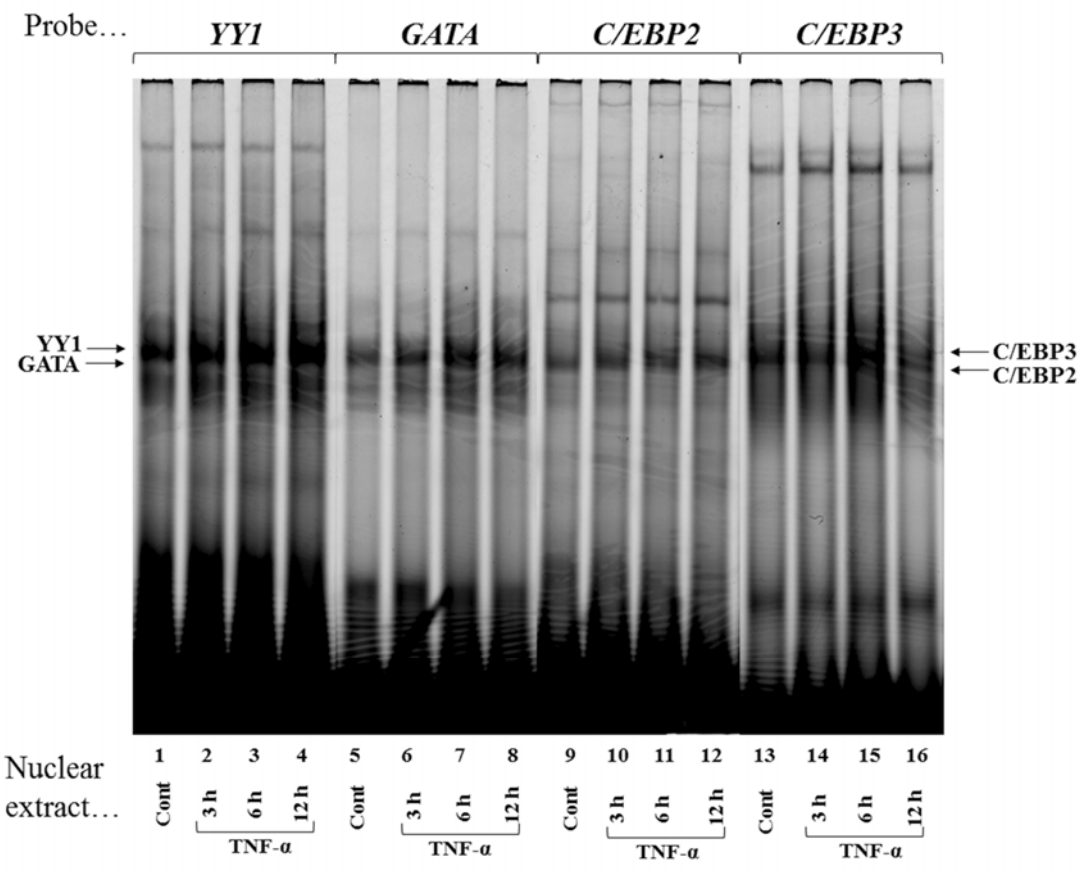

Fig. 7 TNF-α upregulates nuclear proteins that recognize *YY1*, *GATA*, *C/EBP2* and *C/EBP3*. Cy5-labeled double-stranded *YY1*, *GATA*, *C/EBP2* and *C/EBP3* oligonucleotides were incubated with nuclear protein extracts (3 μg) obtained from Ca9-22 cells that were stimulated with TNF-α for 3 h (lanes 2, 6, 10, and 14), 6 h (lanes 3, 7, 11, and 15) and 12 h (lanes 4, 8, 12, and 16) or without TNF-α (lanes 1, 5, 9, and 13). DNA-protein complexes were separated on 5% polyacrylamide gel, and scanned with Typhoon TRIO+ variable Mode Imager.

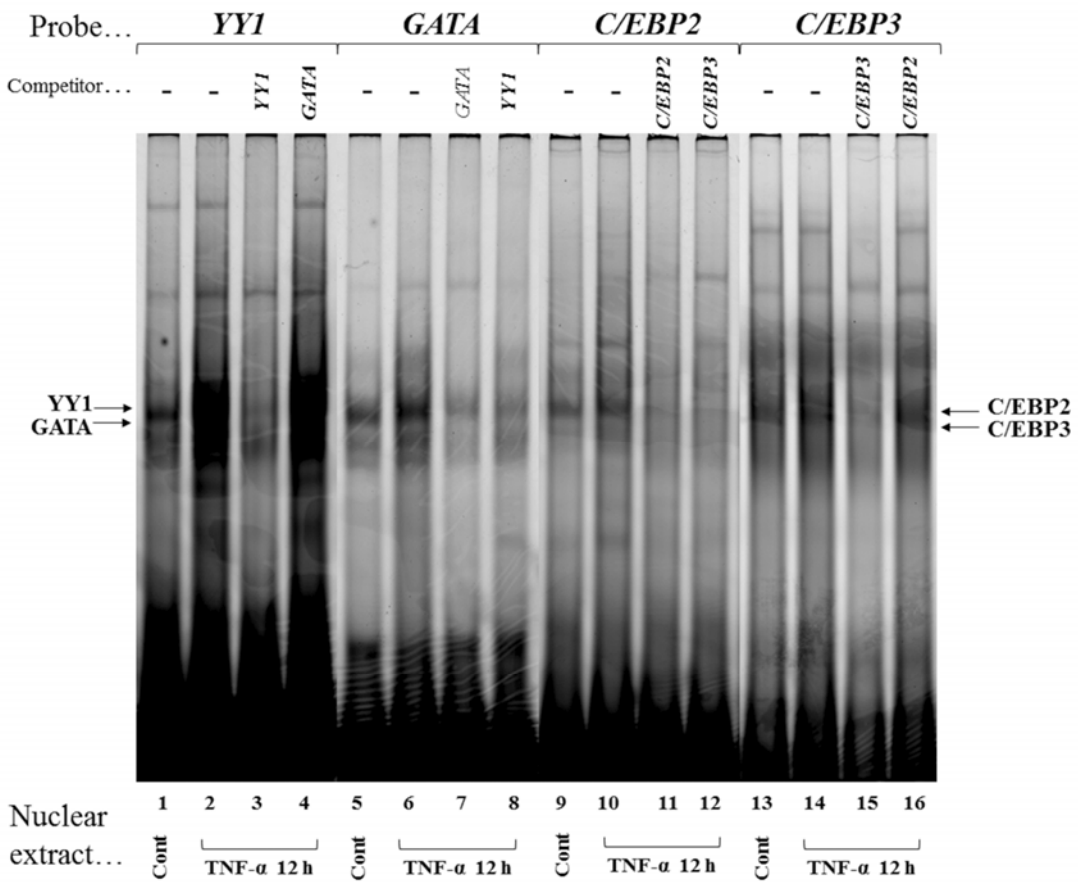

Fig. 8 Specific binding of nuclear proteins to *YY1, GATA, C/EBP2* and *C/EBP3*. Competition assays were performed using 40-fold molar excess of unlabeled *YY1* (lanes 3 and 8), *GATA* (lane 4 and 7), *C/EBP2* (lanes 11 and 16) and *C/EBP3* (lane 12 and 16) oligonucleotides. DNA-protein complexes were separated on 5% polyacrylamide gel, and scanned with Typhoon TRIO+ variable Mode Imager.

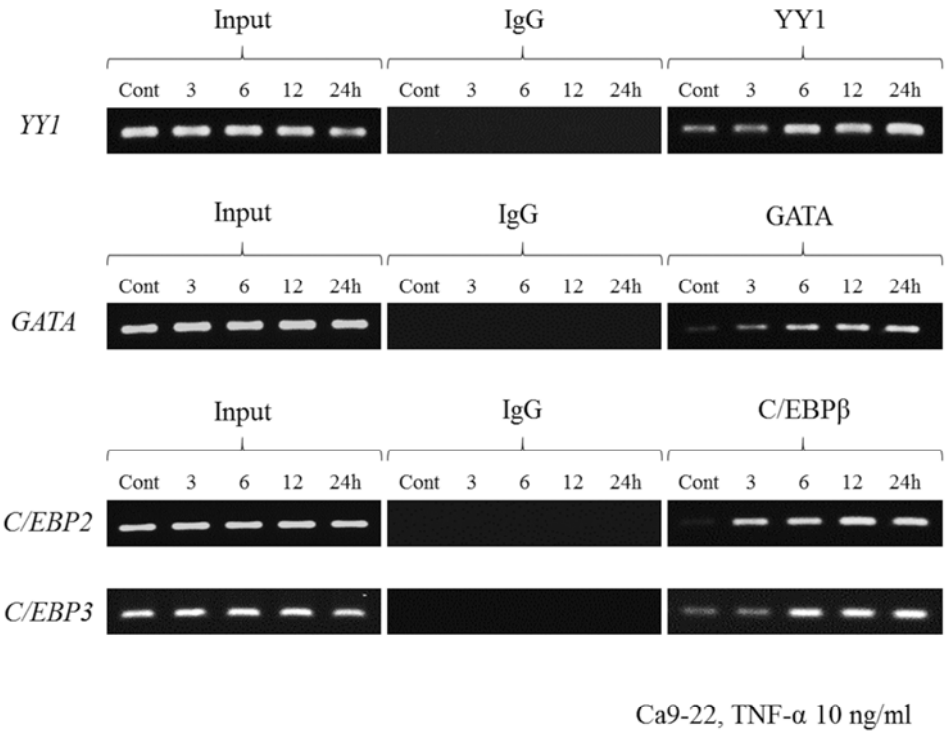

Fig. 9 ChIP analyses of transcription factors binding to *YY1, GATA, C/EBP2* and *C/EBP3* in the human *FDC-SP* gene promoter in Ca9-22 cells. PCR bands amplified and corresponding to DNA-protein complexes immunoprecipitated with antibodies showed that YY1, GATA and C/EBPβ transcription factors interacted with a chromatin fragment containing the *YY1, GATA, C/EBP2* and *C/EBP3*, which were increased in Ca9-22 cells following stimulation with TNF-α (10 ng/ml). Input DNA was also used as a control in PCR analysis.

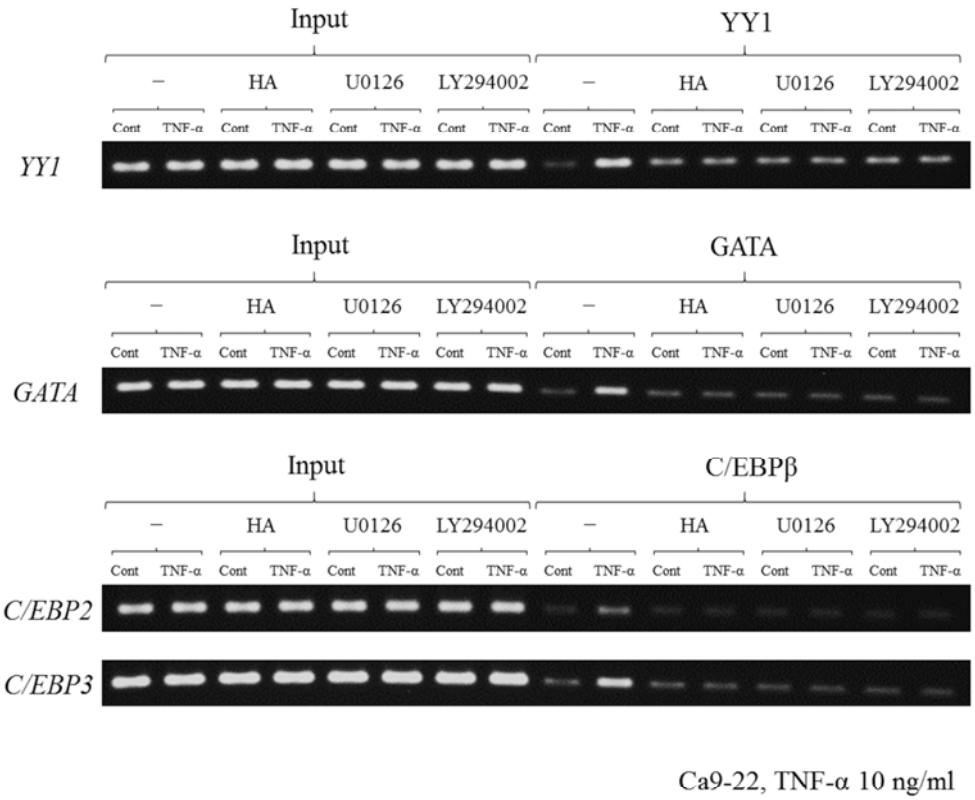

Fig. 10 ChIP analyses of transcription factors binding to *YY1, GATA, C/EBP2* and *C/EBP3* under the treatment by TNF-α (10 ng/ml, 12 h) with kinase inhibitors. Treatments of HA, U0126 and LY294002 almost completely abolished the induction of YY1, GATA and C/EBPβ transcription factors bindings to *YY1, GATA, C/EBP2* and *C/EBP3* by TNF-α.

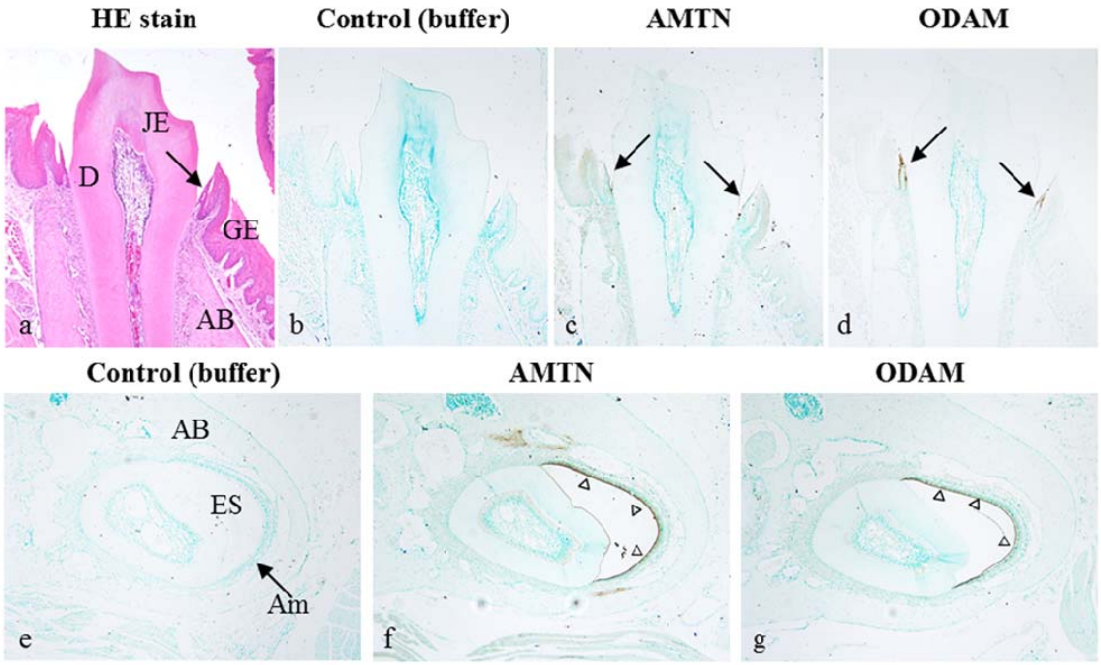

Fig. 11 Localization of AMTN and ODAM in the JE at the second molars (top row) and ameloblasts in the mandibular incisor (bottom row) of mice.

HE staining (a) and Immunostaining (b-g). AMTN and ODAM localization were detected in the JE (as shown by arrows in c and d), but not in the control (b). In the ameloblast of the mandibular incisor, signals of AMTN and ODAM were later shown at the interface between the enamel space and ameloblasts (as shown by arrowheads in f and g). AB; alveolar bone, Am; ameloblasts, D; dentin, ES; enamel space, GE; gingival epithelium, JE; junctional epithelium.

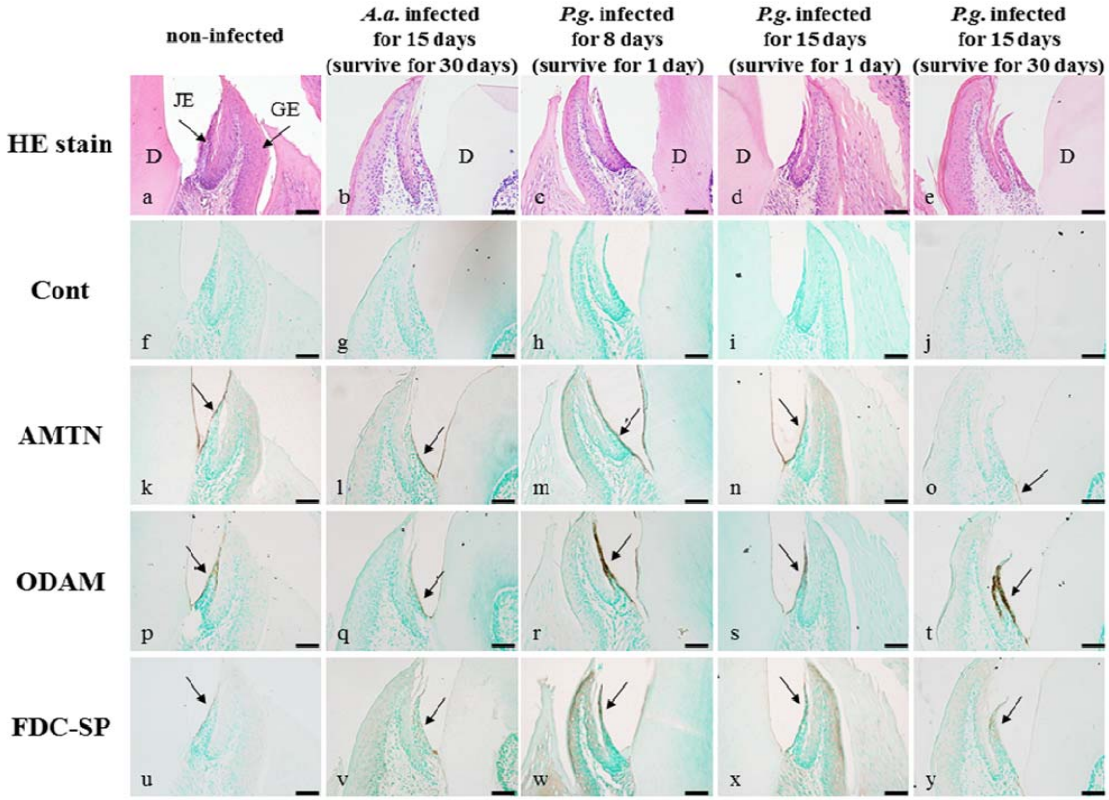

Fig. 12 Localization of AMTN, ODAM and FDC-SP in the JE at the second molars of *A. actinomycetemcomitans* and *P. gingivalis* infected mice.

HE staining (a-e) and Immunostaining (f-y). To determine an alteration of AMTN, ODAM and FDC-SP expression in the *A. actinomycetemcomitans* and *P. gingivalis* infected mice, immunohistological analysis was carried out. AMTN and FDC-SP signals were detected to be stronger in the *P. gingivalis* infected mice [*P. gingivalis* infected for 8 days (survived for 1 day) (m and r) and *P. gingivalis* infected for 15 days (survived for 1 day) (n and s)] compared with non-infected mice (k and u). Localization of AMTN in *P. gingivalis* infected mice [*P. gingivalis* infected for 15 days (survived for 30 days) (o)] was changed at JE associated with the increase of epithelium to apical direction along the root surface, compared to non-infected and *A. actinomycetemcomitans* infected mice (arrow in k and l). However, AMTN, ODAM and FDC-SP expression did not change in the *A. actinomycetemcomitans* (l, q and v) infected mice compared to the control (k, p and u). bars: 50 μm.